

Control System Development and Flight Testing of the Tiger Moth UAV

Brian T. Fujizawa

Mark B. Tischler

Aeroflightdynamics Directorate (AMRDEC)
U.S. Army Research, Development, and
Engineering Command
Moffett Field, CA

Paul E. Arlton

Dave J. Arlton

Lite Machines Corporation
West Lafayette, IN

Abstract

There is a need to provide high-resolution video imagery to the sensor operators of current and future gunships while supporting missions above an area of interest. Sensor operators need to see beyond the visual range of the main platform, peer through weather, and monitor multiple geo-separated or dispersing targets. The Lite Machines Tiger Moth UAV is designed to fill this need. The objective of the work presented herein was to improve the inner loop control laws of the Tiger Moth UAV through control system modeling, optimization and flight tests. Laboratory tests were conducted to identify aircraft sensor and servo dynamics. A bare-airframe hover/low-speed dynamics model was developed from piloted frequency sweeps. The identified components and dynamics model were combined with a Simulink[®] representation of the control laws to form a validated analysis model which was used in CONDUIT[®] to optimize the attitude loop feedback gains. Flight tests with the optimized gains showed improved performance. Finally, the improvements were demonstrated to the U. S. Air Force in untethered flight tests conducted at Camp Atterbury, Indiana, in December of 2011.

Notation

a_x, a_y, a_z	Longitudinal, lateral, and vertical accelerations [m/s ²]
h	Height of point of rotation above the aircraft's center of gravity [m]
I_y	Pitch moment of inertia [kg m ²]
m	Mass of the aircraft [kg]
p, q, r	Roll, pitch, and yaw angular rates [deg/s]
u, v, w	Body velocities [m/s]
$\delta_{lat}, \delta_{lon}$	Roll, pitch, and heave control inputs [deg]
δ_{col}	Differential torque – yaw control input [%]
$\delta_{\Delta Q}$	Differential torque – yaw control input [%]
ϕ, θ, ψ	Roll attitude, pitch attitude, and heading [deg]
$(\)'$	Test stand value with rotation about a pivot point other than the aircraft's center of gravity

Introduction

The Tiger Moth V6.1 UAV (Figure 1) developed by Lite Machines Corporation is an outgrowth of the Voyeur UAV which was developed for the U.S. Navy as a sonochute-launched UAV for use on the Lockheed P-3 Orion and the Boeing P-8 Poseidon. Lite Machines is currently working under a U.S. Air Force Phase III SBIR contract to refine the Tiger Moth V6.1 control system for more extensive air-launched flight tests.

The Tiger Moth is a 3.5 pound, electrically-powered, unmanned helicopter having an 18 inch vertically elongated body with 30 inch diameter, counter-rotating, coaxial rotors that fold for storage inside a tube. Each rotor system is driven by a separate electric motor and includes both cyclic and collective pitch controls which are actuated by a common set of servo actuators located midway between the

Presented at the American Helicopter Society 68th Annual Forum, Fort Worth, TX, May 1-3, 2012. This is a work of the U.S. Government and is not subject to copyright protection in the U.S.

DISCLAIMER: Reference herein to any specific commercial, private, or public products, process, or service by trade name, trademark, manufacturer, or otherwise, does not constitute or imply its endorsement, recommendation, or favoring by the United States Government. The viewing of the presentation by the Government shall not be used as a basis of advertising.

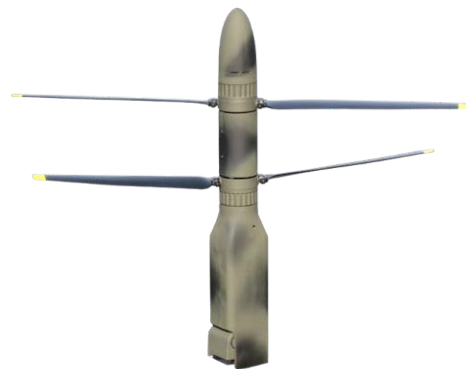


Figure 1. Tiger Moth

rotors. Directional control is achieved using differential rotor torque.

The Tiger Moth airframe consists of a hollow aluminum spine tube extending the full length of the body which acts as both a rigid structural element and a conduit for electrical wiring. Power to drive the rotors is transmitted by electrical wiring running through the spine tube instead of mechanical shafting thereby reducing mechanical complexity and weight. The spine-tube style airframe can withstand high launch loads and has been tested by the Navy to withstand 100 Gs during a sonochute launch.

When configured for hovering flight, the Tiger Moth flies in a near-vertical orientation. A GPS guidance and telemetry system is mounted above the rotors for unobstructed access to the sky. A lower payload module houses sensors including infrared and/or visible-light video cameras, a telemetry system for transmitting digital data back to a command center, and possibly a warhead to disable small vehicles.

The current effort is part of an on-going program sponsored by the Air Force Research Laboratory (AFRL) to develop a disposable, air-launched, off-board sensor for a variety of manned aircraft. The requirements of this program are challenging from a control system perspective. After being ejected from a manned aircraft flying at over 200 knots, the sensor vehicle must fall or fly to a lower altitude, automatically configure itself for flight, then transmit stable sensor imagery to a remote operator for up to one hour. It must travel at high speeds between widely separated waypoints, hover for extended periods of time, and operate in high and gusting winds. While considered disposable by aircraft operators, the vehicle may be hand recovered and reused by ground forces.

This paper describes work jointly performed by Lite Machines and the U.S. Army Aeroflightdynamics Directorate to improve the hover/low-speed performance of the Tiger Moth. The effort involved conducting laboratory tests on individual components as well as the complete aircraft, identifying a state-space model from flight test data, developing and validating an analysis model, and optimizing the control system based on the analysis model. Results of the optimization are discussed and compared with flight test observations. Finally, a brief overview of the Air Force demonstration flight tests is presented.

Laboratory Tests

In order to develop a useful analysis model, it is important to first accurately model all the components of the aircraft. To this end a series of laboratory tests were performed by Lite Machines. Automated frequency sweeps were used to identify the dynamics of the flight sensors and servos actuators. Servo position data was recorded as the servos were commanded to sweep through a range of frequencies. From this data, transfer function models of the servos were

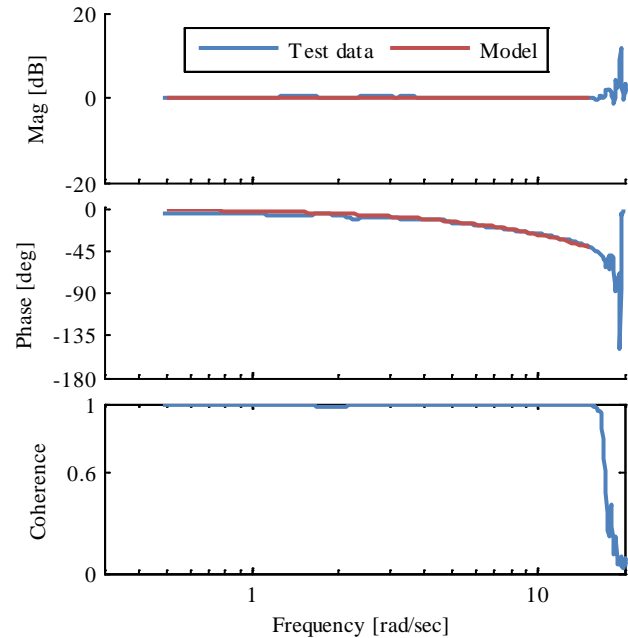


Figure 2. Identified servo transfer function model

developed as shown in Figure 2. A time delay alone ($H = e^{-0.048s}$) was sufficient to model the servos with a cost of $J = 2.2$ which indicates the model is nearly perfect.

Validation of the inertial measurement unit (IMU) sensor was achieved by performing frequency sweeps with the Tiger Moth rotors turning at full speed and mounted on a programmable robotic arm capable of 0.001 degree resolution and rotating the entire airframe and IMU. This produced a more controlled flight environment where the sensor signal noise could be analyzed in the context of airframe and rotor vibration. It was also possible to check the angular kinematic consistency of all IMU data to ensure proper sensor orientation and scale factors. Translational kinematic consistency was verified by mounting the test stand in a car, and driving the car down a road while collecting velocity and acceleration data with the onboard GPS and IMU.

The majority of the laboratory testing during this program was performed on either the single-axis yaw test stand shown in Figure 3a or the fully articulated pitch/roll test stand shown in Figure 3b. All articulated axes were supported by low-friction instrument bearings to ensure high fidelity measurements. Due to the location of the aircraft's center of gravity, it was not possible to clamp the aircraft in the pitch/roll test stand so that rotation occurred about the center of gravity. This was accounted for in the subsequent calculations.

The pitch and roll moments of inertia of the aircraft are identical and were determined by performing a swing test with the aircraft mounted in the pitch/roll test stand [1]. From the damping envelope and damped natural frequency

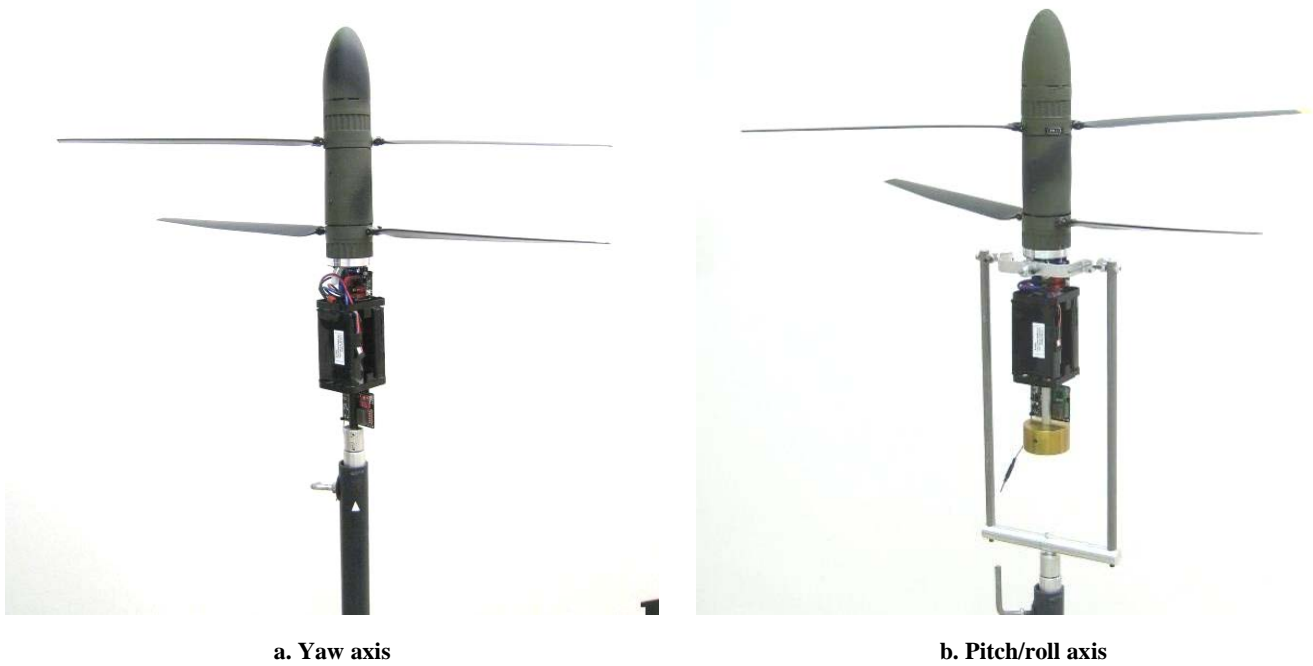


Figure 3. Laboratory test stands

illustrated in Figure 4, it was possible to calculate the undamped natural frequency and thus the inertia. Since the aircraft was clamped in the stand at a point other than the center of gravity, this value was corrected to the aircraft's center of gravity through the use of the parallel axis theorem.

The Tiger Moth's symmetrical construction about the vertical spine results in the aircraft's center of gravity being located along this spine. When mounted in the yaw axis test stand, the spine is clamped in a low friction bearing allowing the aircraft to freely rotate about the vertical axis as it would in flight. Using this setup, it was possible to identify the yaw axis dynamics through frequency sweep data. Using CIFER[®] [2] to identify a frequency response of yaw rate to differential torque, a transfer function of the yaw dynamics

was identified as:

$$\frac{r}{\delta_{\Delta Q}} = \frac{8.852}{s} e^{-0.0592s} \quad (1)$$

Figure 5 compares the flight test data with the identified transfer function model which has a transfer function fit cost of $J = 57.3$. The transfer function fit cost is a metric describing the accuracy of a model and is calculated as the least-squares average of the error between the model gain and phase and the flight data. Costs of less than 100 are considered acceptable while costs below 50 are excellent. A cost of 57.3 indicates that the model accurately represents the yaw axis dynamics.

A similar attempt was made to identify the pitch and roll axis dynamics from frequency sweeps performed on the test stand. Equations of motion were derived in order to account for the fact that the aircraft did not rotate about the center of gravity while on the stand. For example, an estimate of the "free-flight" M_q (i.e. the M_q which would be identified from flight test data) in terms of test stand quantities is given by:

$$M_q = \frac{I'_y}{I_y} M'_q - \frac{mh}{I_y} X'_q \quad (2)$$

where the prime notation indicates test stand values with rotation about some point other than the center of gravity. This attempt proved unsuccessful as the COTS force sensors on the test stand included low-pass filters and so were ineffectual at capturing the dynamic force response during a frequency sweep. This force response is needed to determine the second term (X_q) in the above equation.

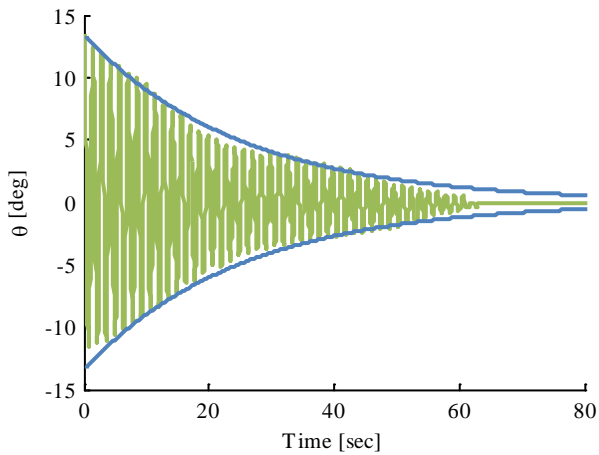


Figure 4. Pitch attitude response during swing test

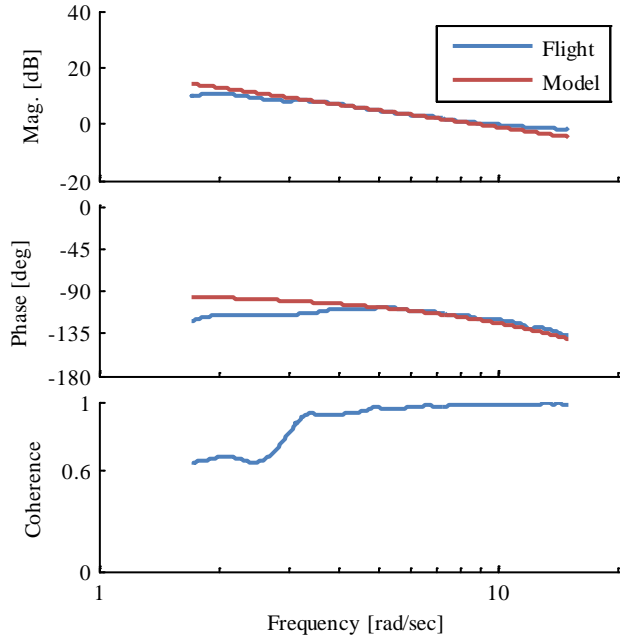


Figure 5. Yaw axis identified transfer function model

While it was not possible to calculate the dynamic response in the pitch or roll axes, it was possible to analyze the steady-state response. From this, it was possible to calculate the speed damping derivative, X_u which can be very difficult to identify from frequency sweep data. Using a large fan positioned some distance from the aircraft, it was possible to simulate low-speed, steady-state flight on the test stand. The fan was set to several different airspeeds as measured by a hot-wire anemometer near the aircraft. The steady state forces were measured by load cells on the test stand, then the forces were rotated from the test stand frame into the body frame. The body X-force vs. airspeed data is plotted in Figure 6 and fit with a least-squares line. The derivative X_u is calculated as:

$$X_u = \frac{1}{m} \left(\frac{\Delta X}{\Delta u} \right) \quad (3)$$

where $\Delta X/\Delta u$ is the slope of the line in Figure 6. Using this equation along with the slope of the trend line and the aircraft's mass, the speed damping derivative was calculated to be $X_u = -0.0519 \text{ sec}^{-1}$. This value was fixed in the flight identified model (Table 1).

Proposed improvements to the pitch/roll test stand force sensors should improve the steady-state data as well as make it possible to identify the dynamic force response.

Model Identification from Flight Tests

A bare-airframe dynamics model was developed for the Tiger Moth using the system identification techniques described in [2] and free-flight data. These techniques have previously been applied to successfully develop models of several different UAVs [3][4][5]. First, frequency sweep

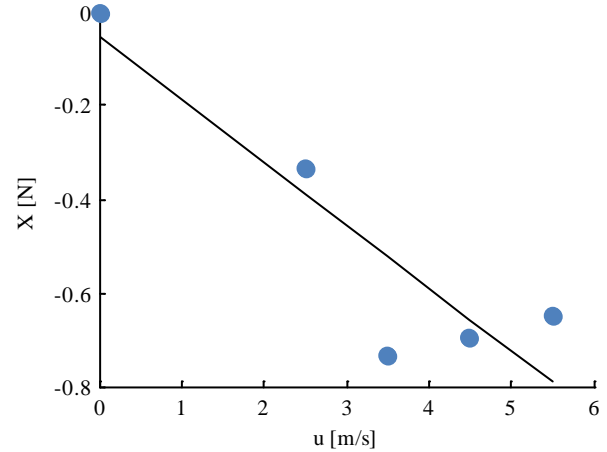


Figure 6. Longitudinal trim force data

and doublet flight test data is collected in each axis. Then, the frequency sweep data is used to identify the individual frequency responses and state-space dynamics model. Finally, the doublet data is used to validate the identified model in the time domain.

Outdoor flight tests were conducted at a local soccer field with the vehicle anchored to the ground by a lightweight Kevlar tether as a safety measure. While the tether was light enough not to impact the aircraft dynamics, it could snag on irregularities as it dragged along the ground causing uncommanded inputs to affect the flight data. Flight testing over freshly mowed grass significantly improved the quality and reliability of the test data.

Initially, it was difficult to perform frequency sweeps without feedback (i.e. open loop) due to the natural instabilities of the aircraft response. Without an active stabilization system the pilot was able to control the aircraft for only a few seconds. In order to perform the needed frequency sweeps, the control system's pitch and roll gains were adjusted by hand until sufficient damping was achieved. Even so, significant pilot concentration and restraint was required to avoid overturning the vehicle at sweep frequencies near the airframe natural frequency.

As a result of its slender body configuration, the Tiger Moth has virtually no natural yaw damping which created difficulties in identifying the directional axis dynamics. Initial yaw sweeps were performed on the yaw test stand using a nominal rotor torque difference of 1.5% of hover torque which produced yaw rates in excess of 600 deg/sec. A small amount of derivative gain was needed to artificially damp the pilot's controls during the yaw sweep flights and limit maximum yaw rates to approximately 60 deg/sec.

After collecting sweep data about all axes, CIFER[®] was used to identify a six degree-of-freedom, hover/low-speed, bare-airframe, state-space dynamics model. Due to the aircraft's symmetrical configuration, it was assumed that the dynamics

Table 1. Final identified parameter values

Param.	Value	CR %	Insens. %
X_u	-0.0519 ^a		
X_q	-0.1941	8.8433	3.6587
Z_w	-0.2241	15.9580	7.3478
M_u	3.4916	5.8704	1.2765
M_q	-3.4370	9.4356	2.2425
N_r	0 ^b		
X_{lon}	0.1094	12.3481	5.6205
Z_{col}	-0.8333	5.0609	2.3303
M_{lon}	5.2252	4.4206	1.2867
$N_{\Delta Q}$	8.3679	4.1343	2.0671
τ_{lon}	0.0961	8.5677	3.2266
τ_{col}	0 ^b		
$\tau_{\Delta Q}$	0.0684	9.5789	4.7894

^a Fixed parameter in model structure

^b Eliminated from model structure

of each axis was decoupled from the others and that the pitch and roll dynamics were identical save the necessary sign differences.

Table 1 presents the values of the identified parameters as well as their Cramér-Rao bounds and insensitivities. The low Cramér-Rao bounds (< 20%) and insensitivities (< 10%) indicate that the identified parameters are reliable [2]. Additionally, the low individual and average overall transfer function costs ($J_{ave} = 63.7$) presented in Table 2 and the frequency domain comparison of the model and the flight data illustrated in Figure 7 show that the identified model is an accurate representation of the aircraft dynamics.

The two directional axis parameters in Table 1 ($N_{\Delta Q}$ and $\tau_{\Delta Q}$) closely match the transfer function values identified from the laboratory tests as seen by comparison with Eq. 1. This agreement shows that it is possible to use the test stands to develop an accurate model in the lab and with improvements to the pitch/roll axis test stand force sensors, it should be possible to identify the pitch and roll dynamics through laboratory testing as well.

Time domain validation data is presented in Figure 8 for the longitudinal axis (roll axis would be the same) and Figure 9 for the heave axis. The figures show good agreement between the flight data and the model in both axes.

Table 3 presents the associated time domain validation metrics for these responses. The rms fit error (J_{rms}) is a

Table 2. Identified model costs

Response	Cost
u/δ_{lon}	78.80
q/δ_{lon}	73.60
a_x/δ_{lon}	61.31
w/δ_{col}	33.38
$r/\delta_{\Delta Q}$	71.41
Average	63.70

Table 3. Time domain validation metrics

Input	J_{rms}	TIC
δ_{lon}	3.662	0.115
δ_{col}	0.581	0.211

weighted rms error between the flight data and the model data with a suggested weighting of: 1deg = 1deg/sec = 1ft/sec = 1ft/sec² (see [2]). An acceptable level of accuracy using this weighting is $J_{rms} < 1$ to 2. This guideline is based on an input calibrated to give a primary response with a magnitude of 10, e.g. for a longitudinal input, the desired pitch rate is 10 deg/sec. Figure 8 shows that the pitch rate response is nearly 80 deg/sec, far greater than the desired 10 deg/sec rate, and the rms fit cost of Table 3 exceeds the guideline. However, if the guideline is converted to a percentage of the primary response, (i.e. $J_{rms} < 10\%$ to 20% of primary response), the value presented in Table 3 is well within this range (i.e. $3.662 / 80 = 4.6\%$).

Another time domain metric is the Theil inequality coefficient (TIC) [2] which is a normalized parameter used to evaluate the predictive accuracy of the model. The suggested guideline for the TIC is $TIC < 0.25$ to 0.30 , which is well met in both axes.

The signs associated with the two X-force derivatives (X_q and X_{lon}) in Table 1 were unexpected. For a single rotor helicopter with an articulated flapping hinge or small equivalent hinge offset, it is expected that X_q will have a positive sign. This is due to the rotor flapping forward and the associated forward tilt of the thrust vector for a positive pitch rate (pitch back). For a positive longitudinal cyclic input (aft stick commands pitch up) the tip path plane is expected to deflect aft resulting in an aft X-force and thus a negative sign for X_{lon} . Since the frequency domain and time domain metrics indicate that the identified model is accurate, it was assumed that these identified derivatives were “effective” derivatives over the frequency range for which the accelerometer data was available and reflect the dynamics of this coaxial configuration.

From the configuration of the aircraft, it was expected that M_u would be larger for the Tiger Moth than for a single main rotor/tail rotor aircraft, however, the identified value was significantly larger than anticipated. This large value of M_u results in a relatively fast, unstable, oscillatory mode with a natural frequency of $\omega_n = 2.67$ rad/sec and a time to double of $T_{double} = 1.06$ sec. Figure 10 presents a time vector plot [6] of the Phugoid mode. The time vector plot is based on the eigenvectors of the mode and illustrates the relative contribution of each term to the equations of motion. From the figure, it can be seen that M_u provides a significant contribution to the pitch response, in fact, the contribution is greater than that of M_q which is not usually the case. This large value of M_u and the resulting unstable mode was addressed during control system optimization.

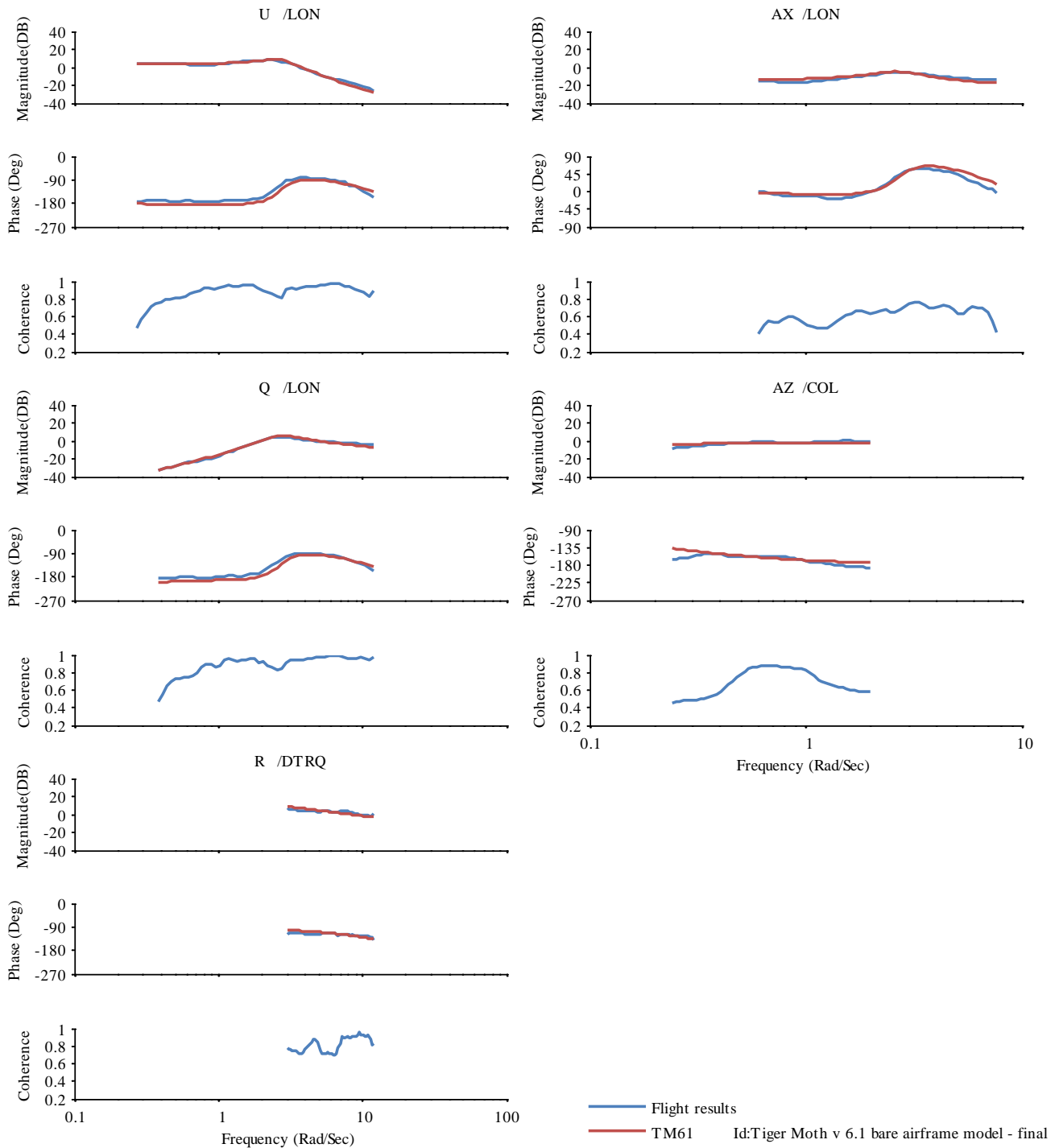


Figure 7. Frequency domain validation of bare-airframe dynamics model

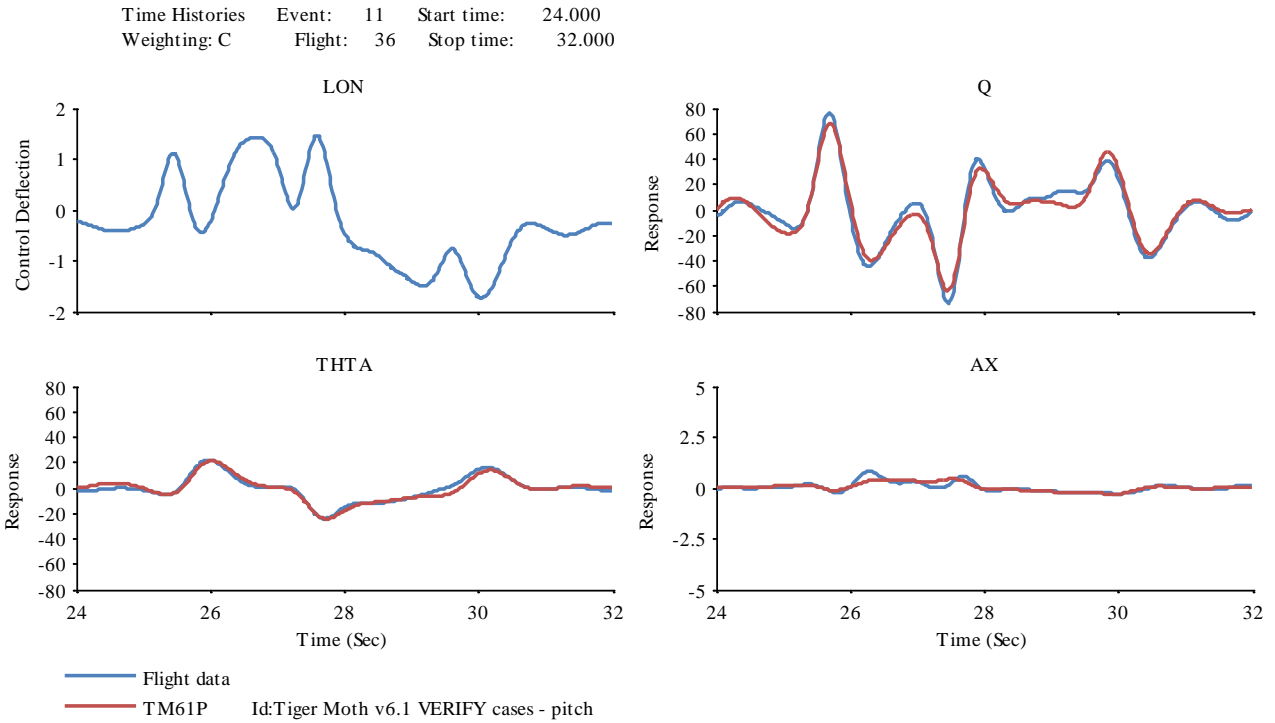


Figure 8. Time domain validation of identified model for a longitudinal input

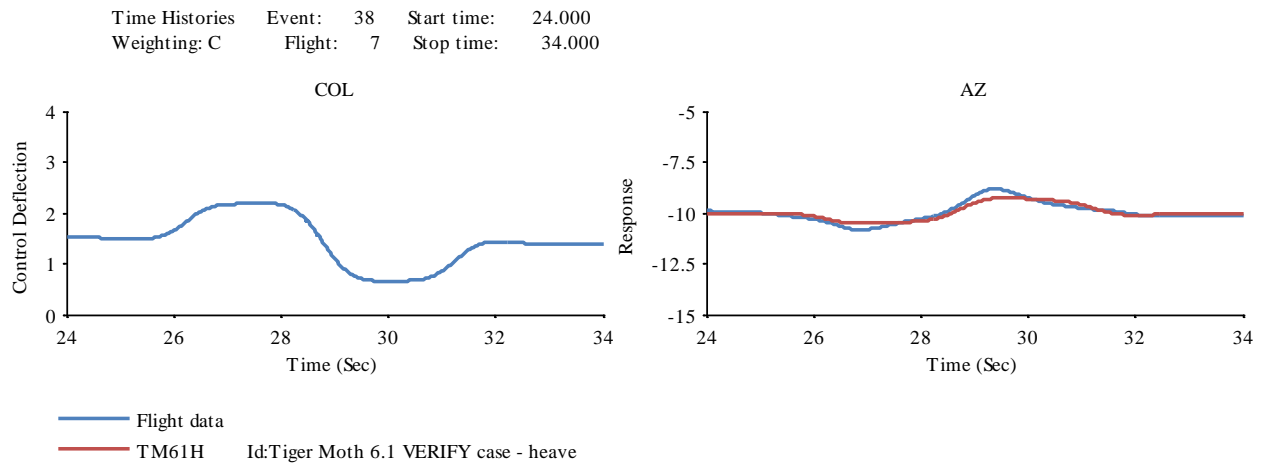


Figure 9. Time domain validation of identified model for a collective input

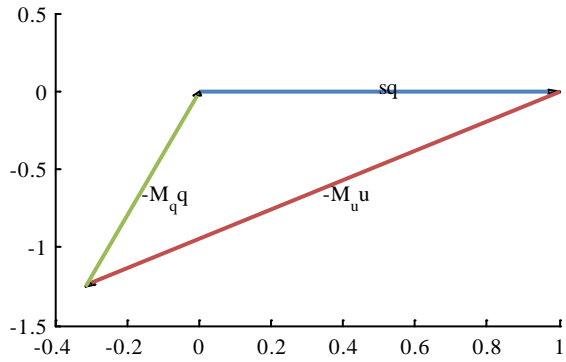


Figure 10. Pitch equation time vector for Phugoid mode

Analysis Model Development and Validation

The analysis model combines the bare-airframe dynamics model identified from flight test data, and the sensor and servo models identified from the bench tests, with a Simulink[®] block diagram representation of the control system for use in CONDUIT[®], a software package used for multi-objective design and optimization [7]. Before performing analysis or optimization, it was necessary to validate the integrated model to ensure that it accurately simulated the actual aircraft behavior. The following paragraphs present the methods used to validate the analysis model. It is important to note that the gains used for the validation were hand tuned gains which allowed test data to be collected, not the optimized gains.

Figure 11 compares the control system pitch command signal of the analysis model with the equivalent signal from the flight data. To generate the analysis signal, all the aircraft state measurements from flight data were fed into the analysis model and the resulting command signal calculated. The good agreement between the flight data and analysis model in the figure indicates that the analysis model has an accurate representation of the feedback control system. Similar tests performed in the other axes produced similarly

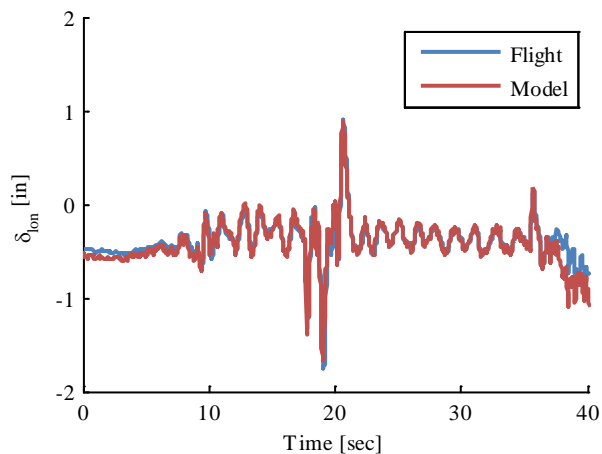


Figure 11. Pitch axis feedback validation

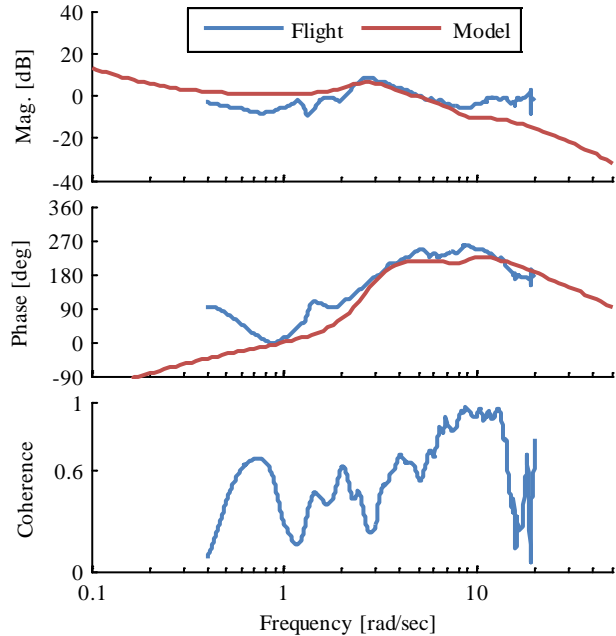


Figure 12. Pitch axis broken loop validation

good agreement.

The next step was to validate the entire analysis model. Figure 12 compares the pitch axis broken loop frequency response identified from automated frequency sweep flight test data with the broken loop response as calculated by CONDUIT[®]. The figure shows good agreement between the flight data and the analysis model over the frequency range of 2 to 9 rad/sec which is the primary frequency range of interest for inner loop flight control design. Good agreement of the broken loop responses indicates that the stability margins and crossover frequencies predicted by the analysis model will be accurate.

Finally, Figure 13 compares the closed loop pitch attitude response of the analysis model with flight data. In a similar

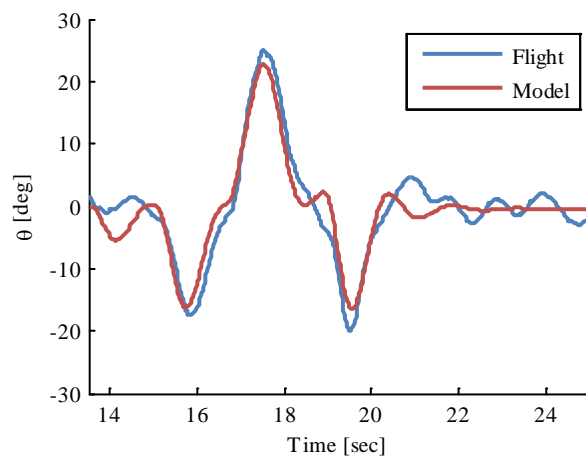


Figure 13. Pitch axis closed loop validation

manner to the feedback validation, pilot inputs from flight test data were fed into the analysis model and the aircraft states were recorded. As with the feedback and broken loop validations, the analysis model shows good agreement with the flight data; the model accurately captures the peaks of the response at 16 sec, 17.5 sec and 19.5 sec.

The results of the validation in the time and frequency domains show that the analysis model accurately represents the actual aircraft. This model can be used reliably in CONDUIT[®] for optimization of the inner loop feedback gains.

Control System Optimization

The inner (attitude) loop of the Tiger Moth control system was optimized in CONDUIT[®] against a comprehensive set of stability and performance specifications, listed in Table 4. The specifications were selected to provide the best possible performance while maintaining sufficient aircraft stability [8].

As mentioned previously, the large value of M_u resulted in an unstable mode in the bare airframe response. In order to achieve a stable closed loop system, it was necessary to select control system gains such that the resulting crossover frequency was higher than the frequency of this unstable mode. However, due to the system's inherent time delay, increasing the crossover frequency reduced the phase margin placing an upper boundary on the crossover frequency. In the final design, it was necessary to accept a slightly reduced phase margin in order to achieve the desired closed loop response.

The Tiger Moth flight controller firmware was modified to include the optimized CONDUIT[®] gains and a series of flight tests were conducted to exercise the new gains under various conditions. It was immediately apparent that stability and control had improved in all axes, especially yaw.

Yaw control of the Tiger Moth had long been a problem due to the low body inertia and powerful rotor torque controls.

Table 4. Tiger Moth control law optimization specifications

CONDUIT [®]	
name	Description
EigLcG1	Eigenvalue location
StbMgG1	Gain and phase margin
StbDaG1	Gain and phase margin from frequency sweep data
EigDpG1	Generic damping ratio from eigenvalues
CrsMnG1	Minimum crossover frequency
DstBwG1	Disturbance rejection bandwidth
DstPkG1	Disturbance rejection peak
TrbAcG1	Actuator rate rms in moderate turbulence
CrsLnG1	Crossover frequency
RmsAcG1	Actuator rms

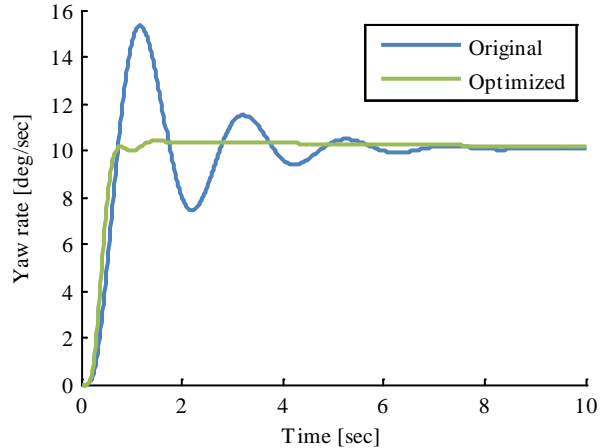


Figure 14. Gain comparison for a directional step

Before developing the analysis model of the system, it had been difficult to hand tune the proportional and derivative gains during outdoor flight tests because high yaw rates associated with an unbalanced system could exceed the sensing limits of the IMU. Figure 14 compares a step response with the original gains and the optimized gains. The step responses were generated using the validated analysis model. The figure shows that the original gains generated a 53% overshoot which was lightly damped ($\zeta = 0.20$). The optimized gains show a better response with very little overshoot and nearly critical damping ($\zeta = 0.92$). This improvement in performance was demonstrated in the final flight demonstration.

Flight Test Demonstrations

Tiger Moth acceptance tests were conducted by government personnel in December, 2011, at Camp Atterbury, Indiana (Figure 15). An important goal of the tests was to demonstrate stable flight as predicted by CONDUIT[®] and validate the control system flight laws.

Weather conditions during the testing were cold (36°F) and overcast with light to moderate winds (2-10 knots). Since all flight tests were conducted in the restricted airspace of Camp Atterbury, it was not necessary to use a tether. Also, to allow easy access to the batteries between flights, the Tiger Moth was flown without the lower body shells. The change in mass was small, and there was no noticeable change in performance with the shells removed.

Test vehicles were controlled with the Tiger Moth Ground Control Station (GCS) V3.2 which included both joystick and waypoint control modes. All flights began with a hand launch to a fixed waypoint whereupon the test vehicle demonstrated stable GPS position and altitude hold. The GCS operator then commanded the test vehicle to transition between velocity-hold and position-hold modes at various altitudes and several waypoints. Throughout all flights the heading remained steady with no noticeable instabilities or yaw excursions. Pitch/roll cyclic controls were orthogonal



Figure 15. Demonstration flight at Camp Atterbury, Indiana

and the test vehicles hovered and transitioned smoothly between waypoints. Flights concluded with a hand recovery at or near the original launch location.

The Tiger Moth UAV system met all contractual requirements for stability and control authority and the flight test results were accepted by the government.

Concluding Remarks

This paper documents the modeling and optimization work performed on the inner loop control laws of the Tiger Moth V6.1 UAV which resulted in improved aircraft performance. Models of the aircraft sensors, servos, and bare airframe dynamics were identified from frequency sweep data. An analysis model was developed and validated in the time and frequency domains. Inner loop feedback gains were optimized and flight tested, showing improved hover/low-speed performance. From this work, the following remarks can be made:

1. Control system development for small scale UAVs is challenging without a validated analysis model due to the combination of low body inertia and powerful controls.
2. It is important to perform sensor validation and data consistency checks early in modeling process to ensure flight test data is accurate and reliable.
3. The use of system identification techniques to identify flight validated models enabled the development of an improved control system.

4. With suitable laboratory test stands, it should be possible to collect sufficient data to develop accurate dynamics models from laboratory testing alone allowing modeling and optimization work to progress before the vehicle is sufficiently developed for safe free flight.

Acknowledgements

The authors wish to thank Sean Henady for his piloting skill and technical support in building and maintaining the Tiger Moth test vehicles. Sean's tireless enthusiasm and dedication were greatly appreciated.

References

- [1] Soulé, H. A. and Miller, M. P., "The Experimental Determinations of the Moments of Inertia of Airplanes," NACA Report No. 467, 1933.
- [2] Tischler, M. B. and Remple, R. K., *Aircraft and Rotorcraft System Identification: Engineering Methods with Flight Test Examples*, AIAA, Virginia, 2006.
- [3] Lipera, L., Colbourne, J. D., Tischler, M. B., Mansur, M. H., Rotkowitz, M. C., and Patangui, P., "The Micro Craft iSTAR Micro Air Vehicle: Control System Design and Testing," Presented at the AHS 57th Annual Forum, Washington, DC, 2001.
- [4] Downs, J., Prentice, R., Dalzell, S., Besachio, A., Ivler, C. M., Tischler, M. B., and Mansur, M. H., "Control System Development and Flight Test Experience with the MQ-8B Fire Scout Vertical Take-Off Unmanned

Aerial Vehicle (VTUAV),” Presented at the AHS 63rd Annual Forum, Virginia Beach, VA, 2007.

- [5] Mansur, M. H., Tischler, M. B., Bielefield, M. D., Bacon, J. W., Cheung, K. K., Berrios, M. G., and Rothman, K. E., “Full Flight Envelope Inner-Loop Control Law Development for the Unmanned K-MAX[®],” Presented at the AHS 67th Annual Forum, Virginia Beach, VA, 2011.
- [6] McRuer, D., Ashkenas, I., and Graham, D., *Aircraft Dynamics and Automatic Control*, Princeton University Press, New Jersey, 1973.
- [7] Tischler, M. B., Colbourne, J. D., Morel, M. R., Biezad, D. J., Levine, W. S., and Moldoveanu, V., “CONDUIT – A New Multidisciplinary Integration Environment for Flight Control Development,” Presented at the AIAA Guidance, Navigation, and Control Conference, New Orleans, LA, 1997.
- [8] Tischler, M. B., Ivler, C. M., Mansur, M. H., Cheung, K. K., Berger, T., and Berrios, M., “Handling Qualities Optimization and Trade-offs in Rotorcraft Flight Control Design,” Presented at the Royal Aeronautical Society Rotorcraft Handling Qualities Conference, Liverpool, UK, November 4-6, 2010.